JACS
JOURNAL OF THE AMERICAN CHEMICAL SOCIETY

Article

pubs.acs.org/JACS

Understanding and Promoting the Rapid Preparation of the *Triplite*-Phase of $LiFeSO_4F$ for Use as a Large-Potential Fe Cathode

Mohamed Ati,[†,‡] Mariyappan Sathiya,[†,‡] Sylvain Boulineau,[†] Marine Reynaud,[†,‡] Artem Abakumov,[§] Gwenaelle Rousse,[∥] Brent Melot,[⊥] Gustaaf Van Tendeloo,[§] and Jean-Marie Tarascon*[,†,‡]

[†]Laboratoire de Réactivité et Chimie des Solides, UMR CNRS 7314, Université de Picardie Jules Verne, 33 rue Saint-Leu, 80039 Amiens Cedex, France

[‡]ALISTORE-European Research Institute, 80039 Amiens Cedex, France

[§]EMAT, University of Antwerp, Groenenborgerlaan 171, B-2020 Antwerp, Belgium

[∥]Institut de Minéralogie et de Physique des Milieux Condensés, UMR CNRS 7590, Université Pierre et Marie Curie (UPMC), 4 Place Jussieu, 75252 Paris Cedex 05, France

[⊥]Department of Chemistry, University of Southern California, Los Angeles, California 90089, United States

Supporting Information

ABSTRACT: The development of new electrode materials, which are composed of Earth-abundant elements and that can be made via eco-efficient processes, is becoming absolutely necessary for reasons of sustainable production. The 3.9 V *triplite*-phase of $LiFeSO_4F$, compared to the 3.6 V *tavorite*-phase, could satisfy this requirement provided the currently complex synthetic pathway can be simplified. Here, we present our work aiming at better understanding the reaction mechanism that govern its formation as a way to optimize its preparation. We first demonstrate, using complementary X-ray diffraction and transmission electron microscopy studies, that *triplite*-$LiFeSO_4F$ can nucleate from *tavorite*-$LiFeSO_4F$ via a reconstructive process whose kinetics are significantly influenced by moisture and particle morphology. Perhaps the most spectacular finding is that it is possible to prepare electrochemically active *triplite*-$LiFeSO_4F$ from anhydrous precursors using either reactive spark plasma sintering (SPS) synthesis in a mere 20 min at 320 °C or room-temperature ball milling for 3 h. These new pathways appear to be strongly driven by the easy formation of a disordered phase with higher entropy, as both techniques trigger disorder via rapid annealing steps or defect creation. Although a huge number of phases adopts the *tavorite* structure-type, this new finding offers both a potential way to prepare new compositions in the *triplite* structure and a wealth of opportunities for the synthesis of new materials which could benefit many domains beyond energy storage.

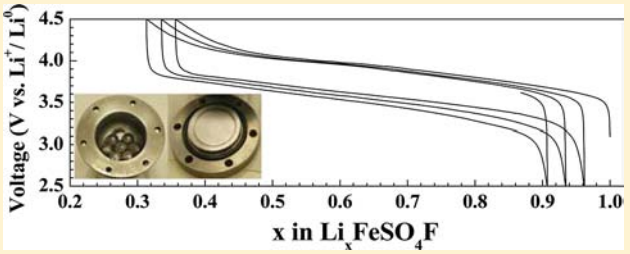

INTRODUCTION

Rechargeable Li-ion batteries power most of today's portable electronics and are serious contenders to facilitate both the development of electric vehicles as well as the widespread use of intermittent renewable energy sources.[1] For this to become reality, limitations in the area of energy density, safety, and manufacturing costs must be overcome; many of which must be addressed at the materials level.[2] Aside from the intrinsic challenges associated with increasing the energy density and cycle life of today's batteries, materials abundance and the environmental side-effects of processing are becoming some of the most pressing issues which must be resolved if Li-ion batteries are to be used in large-volume automotive and grid application markets. This has encouraged the rapid development of Fe-based positive electrodes such as $LiFePO_4$,[3] Li_2FeSiO_4,[4,5] and $LiFeBO_3$[6] which can all be made via environmentally neutral processes.

In pursuing this direction, our group has succeeded in developing new low-temperature routes for the preparation of an entire family of fluorosulfate-based compounds, $AMSO_4F$ (A = Li, Na, K; M = 3d-metal), whose structure strongly depends on the nature of the alkali and transition metals, as well as the reaction conditions.[7−13] Among them, $LiFeSO_4F$ can be prepared in two distinct polymorphs both built upon FeO_4F_2 octahedra and SO_4 tetrahedra, namely, the *tavorite* and the *triplite* structures, which demonstrate significantly different redox potentials when cycled against Li.[8] In particular, the *triplite*-phase of $LiFeSO_4F$ was shown to display both the highest potential ever reported for an Fe-based compound (3.9 V vs Li^+/Li^0), as well as a theoretical energy density which compares favorably to that of $LiFePO_4$ gravimetrically (587 vs 577 Wh/kg)[9] but is slightly less volumetrically (1916 vs 2001 Wh/l). While the $LiFeSO_4F$ phases meet the overarching goal of using abundant elements like iron and sulfur, the way in which they are prepared leaves much to be desired. Typical

Received: August 2, 2012
Published: October 12, 2012

   dx.doi.org/10.1021/ja3074402 | J. Am. Chem. Soc. 2012, 134, 18380−18387

synthetic methods are usually too long, up to several days for solid-state reactions,[10] or very costly when solution routes that use ionic liquids are pursued. Additionally, there are still several issues for the production of high-purity materials.

It has now been well-established that the formation of the *tavorite* phase of $LiFeSO_4F$ proceeds via a topotactic reaction starting from the precursor $FeSO_4{\cdot}H_2O$, through the replacement of water molecules with fluorine atoms that link adjacent FeO_4F_2 octahedra (Figure 1). This synthesis has been

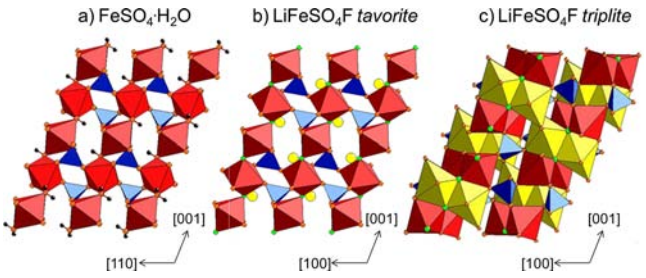

Figure 1. Structures of the precursor $FeSO_4{\cdot}H_2O$ (a), and of *tavorite* (b) and *triplite* (c) $LiFeSO_4F$ polymorphs. SO_4 tetrahedra are blue, hydrogen atoms from H_2O are black, O is orange, and iron sits in the middle of red octahedra. Lithium atoms in *tavorite* are yellow. For *triplite*, iron and lithium are equally distributed over two crystallographic sites M1 and M2, which are located in the middle of the red and yellow octahedra, respectively. Note the structural filiation between $FeSO_4{\cdot}H_2O$ and *tavorite*, whereas no obvious similarities can be seen with the *triplite* polymorph.

extremely optimized and has reached the stage at which it is highly reproducible.[10,11] In contrast, the *triplite*-phase has no structural similarity to $FeSO_4{\cdot}H_2O$, and it was found that a rapid heating rate (10 °C/min) to the reaction temperature of 320 °C was mandatory to prepare single-phased *triplite* from stoichiometric mixtures of $FeSO_4{\cdot}H_2O$ and LiF in sealed Teflon-lined bombs. A direct nucleation of the *triplite* phase from water-free $FeSO_4$ was proposed[9] to account for this finding, but attempts to directly prepare the *triplite* phase from $FeSO_4$ and LiF were never successful. This raised significant questions about the role of water during the synthesis of *triplite* $LiFeSO_4F$.

More recently, a careful investigation of the thermochemistry associated with the iron–manganese *tavorite* and *triplite* phases using solution calorimetry revealed that the formation of disordered *triplite* structure was enthalpy disfavored yet entropically stabilized, suggesting that synthetic pathways leading to disorder should favor *triplite*.[12] Indeed, in *triplite* iron and lithium atoms are statistically distributed between two crystallographic sites, M1 and M2, both of which are octahedrally coordinated by four oxygen and two fluorine atoms which sit in *cis* positions with respect to each other (Figure 1c). These thermochemical results gave a strong impetus to revisit the preparation of *tavorite* and *triplite* polymorphs via ceramic and ionothermal preparations so as to further explore the optimal pathway for the preparation of the *triplite* phase.

Herein, we demonstrate the feasibility of (i) transforming *tavorite* into *triplite* with extended annealing, thus confirming the previous report by Nazar's group[13] and (ii) synthesizing electrochemically active and single-phased *triplite* $LiFeSO_4F$ by simply reacting $FeSO_4$ with LiF using either room-temperature reactive ball milling for 3 h or spark plasma sintering (SPS) synthesis[14] in less than 20 min at 320 °C. Additionally, we successfully implemented the SPS technique to the elaboration of other attractive fluorosulfates ($KMSO_4F$)[15] or lithium iron sulfate $Li_2Fe(SO_4)_2$[16] electrode materials.

EXPERIMENTAL METHODS

a. X-ray Diffraction. X-ray diffraction (XRD) patterns were recorded using two separate Bruker D8 diffractometers. The first one was equipped with a Co–K_α radiation source (λ_1 = 1.78897 Å, λ_2 = 1.79285 Å) with a Vantec detector, while the other used a Cu–K_α radiation source (λ_1 = 1.54056 Å, λ_2 = 1.54439 Å) with a LynxEye detector. Both were operated at 40 kV and 40 mA. The powder patterns were refined using the Rietveld method[17] as implemented in the FullProf program.[18]

b. Transmission Electron Microscopy (TEM). Electron diffraction (ED) patterns and dark field (DF) TEM images were obtained with a Tecnai G2 electron microscope operated at 200 kV. Samples were prepared in an Ar filled glovebox by crushing the crystals in a mortar in anhydrous ethanol and depositing drops of the suspension onto holey Cu-Carbon grids.

c. Electrochemical Characterization. Electrochemical tests vs. Li were done in Swagelok-type cells. The cells were assembled in an argon-filled glovebox, using a Li metal disk as the negative electrode and a Whatman GF/D borosilicate glass fiber sheet saturated with 1 M $LiPF_6$ in ethylene carbonate (EC) and dimethyl carbonate (DMC) (1:1 w/w) as the electrolyte. The working electrodes were typically made by ball milling powders of $LiFeSO_4F$ with 20% in mass of carbon Ketjen black (or SP) for 20 min. Usually, 6 to 8 mg of the mixed powders was used per cell. Galvanostatic charge–discharge tests were conducted at 20 °C using a "Mac-Pile" or a VMP system (Biologic S.A., Claix, France) operating in galvanostatic mode. Unless otherwise specified, the cells were typically cycled vs. Li^+/Li^0 at 1 Li^+ exchanged per 20 h.

RESULTS AND DISCUSSION

a. Growth of *tavorite* $LiFeSO_4F$. To date, all experimental data from our group have indicated that the presence of $FeSO_4{\cdot}H_2O$ is absolutely necessary to obtain $LiFeSO_4F$ in the *tavorite* structure which we have explained based on the structural affiliation between the precursor phase and the structural framework in *tavorite*.[7] However, a recent report[13] claimed that it was possible to prepare *tavorite* by reacting anhydrous Li_2SO_4 and FeF_2, thereby suggesting that the topotactic reaction pathway is not necessary. We therefore attempted to reproduce this experiment using similar precursors and conditions, while monitoring the degree of reaction with periodic XRD measurements. A large batch of vacuum-degassed anhydrous Li_2SO_4 and water-free FeF_2 precursor powders were mixed together, partitioned into 1 g batches, and placed into five separate Teflon-lined stainless steel autoclaves in the presence of poly(ethylene glycol) (PEG) powders (M_w 2000 $\overline{u}$) as reacting medium. The five autoclaves were all placed in the same furnace at the same time, and the temperature was increased to 230 °C. An autoclave was subsequently removed after 2, 5, 10, 35, and 50 h, the powders recovered, and XRD patterns collected. We found that the sample which was reacted for 50 h (Figure 2 bottom XRD pattern) showed the formation of *tavorite* $LiFeSO_4F$ with small amounts of some unidentified impurities. In contrast, the XRD patterns for the samples that were reacted for 2 and 5 h revealed, to our surprise, the presence of $FeSO_4{\cdot}H_2O$. In fact, this monohydrate phase actually becomes the dominant phase in the sample that was reacted for 5 h (Figure 2 middle XRD pattern). Given this data, it appears that water is somehow introduced into the reaction mixture: either from the highly hydroscopic precursors or, more likely, from the PEG where

dx.doi.org/10.1021/ja3074402 | J. Am. Chem. Soc. 2012, 134, 18380–18387

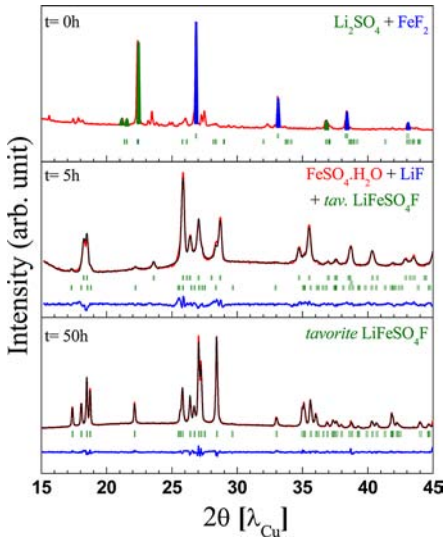

Figure 2. XRD powder patterns showing the evolution of the precursor mixture Li_2SO_4 + FeF_2 (top) placed in Teflon liner bombs in the presence of PEG as a function of the heating duration treatment at 230 °C. Note the formation of $FeSO_4{\cdot}H_2O$ after 5 h of reaction (middle panel) which then transformed in pure *tavorite* after a longer annealing time (50 h, bottom panel), as shown through their Rietveld refinements.

the initial water content was estimated to be around 1200 ppm from Karl Fischer measurements. To test this hypothesis, a pellet of FeF_2 and Li_2SO_4 was loaded into a stainless-steel autoclave fitted with a copper O-ring inside an Ar-filled drybox, and heated at a rate of 1.5 °C/min to 290 °C. After five days of annealing at 290 °C, the powder was found to contain multiple phases (see Figure 3) with two of the major phases being *triplite* $LiFeSO_4F$ and the recently reported $Li_2Fe(SO_4)_2$ phase[16] but with no trace of *tavorite*. Both experiments highlight and reiterate the fact that the monohydrate precursor is critical for the preparation of the *tavorite* phase, and further support the topotactic reaction mechanism proposed earlier.

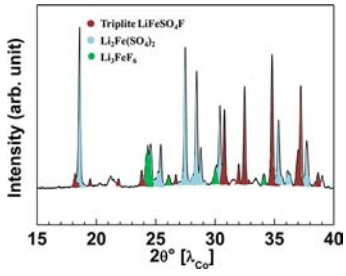

Figure 3. XRD powder pattern of a pellet made from a dried ($FeSO_4$ + FeF_2) mixture which was annealed for 5 days at 290 °C in a stainless steel autoclave filled with Ar. Note that the sample is multiphased with the two main phases being *triplite* $LiFeSO_4F$ and $Li_2Fe(SO_4)_2$ with no sign of *tavorite* $LiFeSO_4F$.

b. Growth of *triplite* $LiFeSO_4F$. Now turning to the *triplite* polymorph, which is the most promising phase for potential applications, the ability to reliably and reproducibly prepare the phase has been a significant challenge. Let's remind that the *triplite* structure is far more complex than the *tavorite* one with two major differences: (i) the Li and Fe atoms are equally and randomly distributed between two M1 and M2 octahedral sites in *triplite*, whereas the octahedral voids are fully occupied by Fe in *tavorite*, and (ii) the (M, Li)O_4F_2 octahedra are highly distorted in the *triplite* polymorph with fluorine atoms sitting in a *cis* orientation rather than in the *trans* orientation as in *tavorite*, and are linked through edges rather than through vertices in *tavorite* (see Figure 1). As a result, there is no clear pathway for lithium diffusion in *triplite*, unlike the wide channels found in *tavorite*. Moreover, the structural similarity observed between the precursor $FeSO_4{\cdot}H_2O$ and the *tavorite* phase is not seen for *triplite*, thereby suggesting that precursors should not be critical to the preparation of *triplite*.

So far, the best way to obtain *triplite* was through a solid-state approach which involves placing a pellet made of thoroughly mixed $FeSO_4{\cdot}H_2O$ with LiF precursors into a Teflon-lined autoclave sealed under an Ar atmosphere and rapidly heated at a high rate of 10 °C/min to 320 °C and annealed for 48 h. In contrast, lowering the heating rate to 5 °C/min was shown to lead to a biphasic powder composed of *tavorite* and *triplite*. It is worth noting that evidence for the transformation of *tavorite* into *triplite* was previously given by Nazar's group by reacting $FeSO_4{\cdot}H_2O$ and LiF in tetra(ethylene glycol) at 230 °C for several days.[13] Therefore, at this stage a legitimate question deals with the feasibility of directly transforming *tavorite* into *triplite* in the absence of water.

To experimentally check this point, a single batch of *tavorite* powder, ionothermally made, was divided into six batches of 800 mg, each one pressed with 5 tons pressure. Three of the resulting pellets were placed in three separate stainless steel autoclaves. The other three were each placed in an alumina crucible which was also placed in a stainless steel autoclave containing 100 mg of $FeSO_4{\cdot}H_2O$ to provide a controlled amount of water in the reacting media. The six autoclaves were then placed in the same oven which was heated to 320 °C in 30 min and maintained at this temperature for several days. Two autoclaves, one containing $FeSO_4{\cdot}H_2O$ and one without, were simultaneously removed after 1 day and the other two pairs after 3 and 6 days, respectively. Once recovered, the pellets were ground and analyzed for phase composition by XRD. The XRD powder patterns coming from the water-containing autoclaves, post-annealing, indicate the formation of a *tavorite*–*triplite* mixture (3 days) and pure *triplite* (6 days) (Figure 4 left). The electrochemical voltage-composition traces for these samples (Figure 4 right) confirm the XRD assignments through the presence of a plateau at 3.6 and 3.9 V, which can be considered as electrochemical fingerprints of the *tavorite* and *triplite* phases for the pristine sample (Figure 4d) and the sample annealed for 6 days (Figure 4f), respectively. In contrast, the potential–composition $V = f(x)$ curve for the sample annealed during three days (Figure 4e) clearly shows the presence of the 3.6 and 3.9 V plateaus implying the coexistence of both phases in approximately equal amounts as deduced from the amplitude of the plateau. A similar molar ratio (*tavorite/triplite*), 40(1)/60(1), within the sample was found in the Rietveld refinement against the XRD powder pattern. The transformation from *tavorite* into *triplite* was also found to occur for the water-free samples, but the kinetics are believed to be slower, since for the same reaction time, the amount of *triplite* obtained is much less (Figure 5). This is indirect evidence that the presence of water facilitates the phase transformation from *tavorite* into *triplite*.

c. The *tavorite*–*triplite* Transformation. To gain further insight into the mechanism of this transformation, transmission electron microscopy (TEM) was collected on a quenched mixture of *tavorite* and *triplite* sample recovered from the

dx.doi.org/10.1021/ja3074402 | *J. Am. Chem. Soc.* 2012, 134, 18380–18387

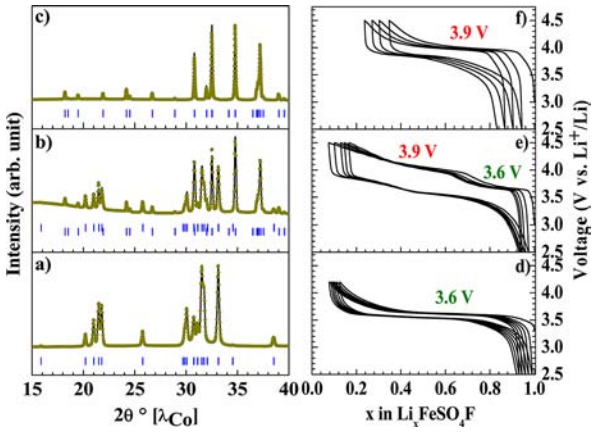

Figure 4. XRD Rietveld refinements showing the *tavorite*−*triplite* transformation upon long annealing at 320 °C in water-containing autoclaves (see text): (a) after one day, the resulting XRD gives a signature of pristine *tavorite*; (b) after 3 days the powder is a mixture of *tavorite* (1st row of green ticks, ∼40%) and *triplite* (2nd row, ∼60%); (c) 100% converted phase into *triplite* after 6 days. On the right panel are displayed the electrochemical performances of the corresponding samples cycled between 2.5 and 4.2 V at a rate of C/20 in (d), and between 2.5 and 4.5 V at the same C-rate in (e) and (f). Note that the capacities for the plateaus at 3.6 V vs Li^+/Li and 3.9 V vs Li^+/Li are in good agreement with the amount of *tavorite* and *triplite* deduced from the Rietveld refinements.

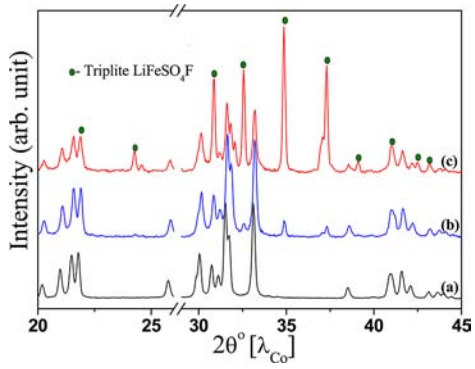

Figure 5. XRD powder pattern of a pristine *tavorite* sample (a) together with the X-ray powder patterns of the same sample once it has been placed in an autoclave and annealed for 3 days at 320 °C without water (b) and in the presence of water (c).

aforementioned experiment (sample b Figure 4 left). To our surprise, in spite of the significant amount of *tavorite* phase in the sample, the electron diffraction patterns from 15 out of the 16 measured crystallites belong to the *triplite* structure and none showed the *tavorite* structure alone. Typical electron diffraction (ED) pattern and dark field (DF) images of the crystallites in the mixed $LiFeSO_4F$ sample are shown in Figure 6a. The DF image reveals that the crystals are inhomogeneous: they contain a darker core surrounded by a matrix of the *triplite* phase, which looks brighter on the images. Since the crystals of this type constitute the overwhelming majority of the sample, one can assume that the particles inside the *triplite* matrix consist of the *tavorite* phase. This suggests that the *tavorite*−*triplite* transformation occurs laterally from the periphery of the crystallite toward its center, so that, when the thinner, outer areas of the crystallite are transformed into the *triplite* structure, the thicker, central part of the *tavorite* is left unchanged. Nevertheless, in one particle (Figure 6b) we have found clear coexistence of both phases, since the ED pattern can be interpreted as a combination of [132] *tavorite* (green) and [10−1] *triplite* (red) ED patterns. The large thickness of these *tavorite* particles makes them nontransparent to electrons explaining the significant contribution of the *tavorite* phase into the XRD pattern and the apparent absence of it in the corresponding ED patterns. In order to provide proof for this assumption, the mixed sample was ball-milled for 2 min and reinvestigated with TEM. After ball-milling, many crystallites demonstrating ED patterns associated with *tavorite* were indeed observed. In many cases, both *tavorite* and *triplite* phases were clearly intergrown within the same crystallite (Figure 6c). It should be mentioned that no high-resolution TEM observations are possible on both *triplite* and *tavorite* phases due to their extreme sensitivity toward electron beam irradiation. Overall, the TEM experiments reveal the presence of particles with a core consisting of *tavorite* and a shell of *triplite* implying a peripheral growth of the *triplite* but do not provide any information regarding the nucleation growth mechanism, as neither specific interfaces nor orientation relationships between *tavorite* and *triplite* $LiFeSO_4F$ could been seen. Nevertheless, from a previous report,[19] the dark field TEM micrographs, with the veil surrounding the core particle (Figure 6a), suggest the feasibility of a process involving local partial dissolution and recrystallization. Besides, phase transformations whose kinetics is affected by the presence of water are also known. For the sake of comparison, one should recall, for instance, that the irreversible hexagonal (h-WO_3) to monoclinic (m-WO_3) phase transformation for WO_3 can be completed at 420 °C in barely five hours if water is present, whereas it takes a full 50 h in a dry atmosphere.[20] Moreover, the difference of ΔH between h-WO_3 and m-WO_3 polymorphs was found to be very small, in the 3−4 kJ/mol range, like the ΔH between *tavorite* and *triplite*; this was explained by common structural features between the two polymorphs.[20] However, like for WO_3, we believe that this transformation is reconstructive rather than displacive, which explains the sluggish kinetics.

While the details of the nucleation and growth mechanism of *triplite* from *tavorite* cannot be determined, several remarks can be made. First, the single crystalline nature (e.g., without planar defects) of the *triplite* shell (see Figure 6a) rules out a phase transition with multiple nucleation centers, since such a scenario would have led to the growth of the *triplite* structure in multiple, and most probably incoherent, orientations to give a twinned microstructure. Regarding the growth mechanism, from the core−shell particle structure observed in microscopy (see Figure 6a), a diffusion process through the transport and diffusion of atoms from the crystal surface toward its interior appears as the most probable. Such a process can proceed either through surface diffusion or via partial dissolution, with the latter being obviously faster compared to surface diffusion processes in the solid state. This could explain the accelerated *tavorite*−*triplite* transformation kinetics in the presence of minute amounts of water. On the contrary, when water is absent, the growth of *triplite* is likely dominated by surface diffusion in the bulk state, hence its dependence on the morphological characteristics of the *tavorite*, namely, its specific surface area, with the slowest transformation for small surface areas samples as we have experienced. Overall, this type of transformation reconciles our experimental observations and literature reports[13] that have evidenced that, once formed, the *tavorite* phase can slowly convert into *triplite* with the

dx.doi.org/10.1021/ja3074402 | J. Am. Chem. Soc. 2012, 134, 18380−18387

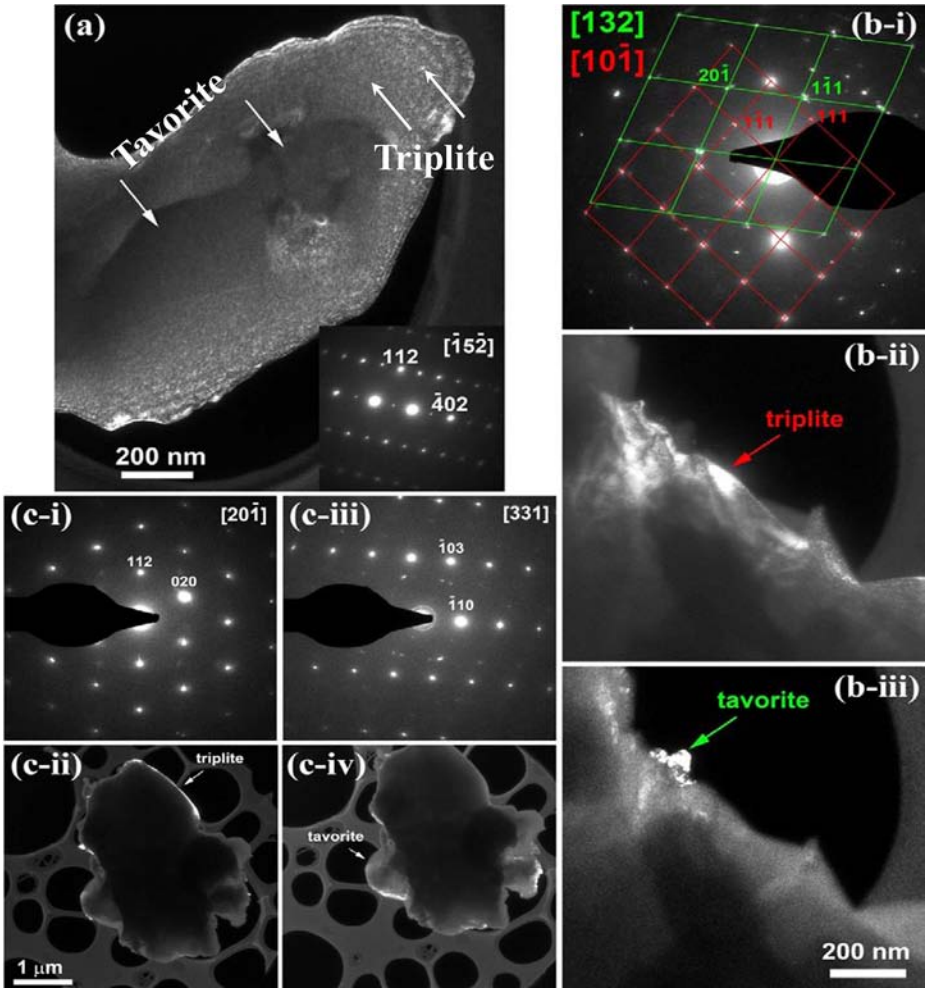

Figure 6. (a) Dark field TEM image of a typical crystallite in the mixed $LiFeSO_4F$ sample. Corresponding electron diffraction pattern is shown in the inset, indexed in the *triplite* lattice. The dark field TEM image taken in a *triplite* reflection demonstrates that the *triplite* phase constitutes the outer area of the crystal (look brighter). The darker particles inside the crystallite (marked with arrows) presumably belong to the *tavorite* phase. (b) Crystallite in the mixed $LiFeSO_4F$ sample showing coexistence of the *triplite* and *tavorite* phases. Electron diffraction pattern (b-i) is interpreted as a combination of the patterns belonging to the *triplite* (red grid) and *tavorite* (green grid) structures. Corresponding dark field TEM images taken in the *triplite* reflection (b-ii) and in *tavorite* reflection (b-iii) demonstrate that the *triplite* and *tavorite* phases form interpenetrating parts of the crystallite. In (c), the ball-milled $LiFeSO_4F$ sample shows the coexistence of the *triplite* and *tavorite* phases. Electron diffraction pattern and dark field TEM images are attributed to *triplite* (c-i, c-ii) and *tavorite* (c-iii, c-iv), respectively. The areas of the crystallite contributing to the corresponding diffraction patterns look brighter and are marked with arrows.

transformation rate being enhanced by the presence of tiny amounts of water.

d. New Synthetic Pathways Toward *triplite* $LiFeSO_4F$. Such an understanding of the *tavorite* to *triplite* phase transformation has motivated us to revisit the direct synthesis of *triplite* phase in autoclaves at 320 °C. This preparation systematically failed when reacting anhydrous $FeSO_4$ with LiF and only succeeded when reacting $FeSO_4{\cdot}H_2O$ with LiF with a quick heating rate. We explained this success as nested in the presence of residual water to facilitate LiF dissociation, thereby enabling a rapid diffusion (e.g., a rapid material transport) which is necessary to stabilize *triplite* $LiFeSO_4F$. However, the failure in the presence of dry precursors is due to the slow atomic diffusion of the reacting species to form *triplite* $LiFeSO_4F$ at temperatures below 340 °C (e.g., its decomposition temperature). These considerations, together with the recent solution calorimetry measurements,[12] which indicated that the phase formation of the *triplite* structure was entropically driven, encouraged the further exploration of the direct synthesis of *triplite* from a dry process by promoting increased atomic diffusion through rapid heating or the introduction of defects. Thus, our motivation to exploit both spark plasma sintering (SPS) and ball milling approaches.

SPS Synthesis. SPS has recently gained a significant amount of attention as a new tool for solid-state chemists and was recently demonstrated to lead to the successful synthesis of Li_2CoPO_4F electrodes.[21] Its unique feature relies on the simultaneous application of high pressure and electric current to a powder sample so that the rate of heat and mass transfer is significantly increased to allow rapid diffusion of atoms.[14,22] Compared with classical ceramic or hot pressing approaches, SPS has the advantage of providing heating in a quick and homogeneous way in order to significantly reduce the reaction time.

The SPS experiments were carried out with an HPD 10 FCT SPS machine installed within an argon drybox so that moisture-sensitive precursors can easily be handled and are capable of reaching pressures and temperatures up to 200 MPa and 2000

dx.doi.org/10.1021/ja3074402 | J. Am. Chem. Soc. 2012, 134, 18380−18387

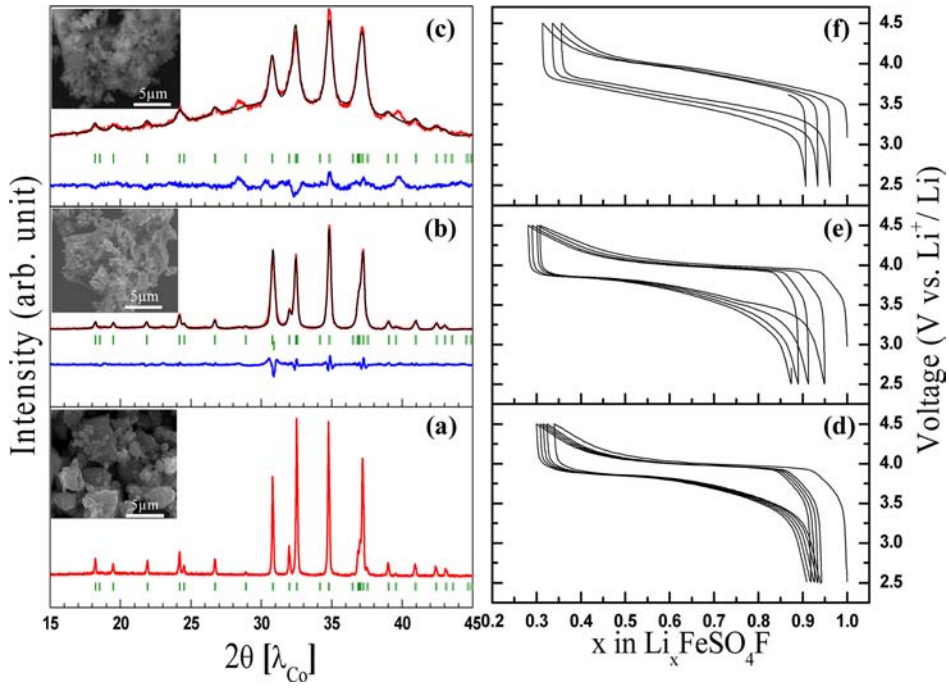

Figure 7. Rietveld refinements of the XRD diffraction patterns of (a) ceramic-made *triplite* $LiFeSO_4F$ as compared with (b) SPS made (15 min at 320 °C) and (c) BM-made (3 h of grinding with a weight ratio of stainless steel balls to powder of 40) ones. Typical SEM images for each sample are shown in the inset. The electrochemical performances for the corresponding samples when cycled at a C/20 rate are shown in (d), (e), and (f).

°C, respectively. For each experiment, stoichiometric amounts of anhydrous $FeSO_4$ powders, made by heating $FeSO_4{\cdot}H_2O$ at 280 °C under primary vacuum for 3 h, and LiF were thoroughly ball milled (1 h) in a Spex 8000 miller and then cold-pressed into a ⌀10 mm pellet under a pressure of 620 MPa. Afterward, the pellet was sandwiched between two carbon paper disks, introduced in a carbon die (Carbone Lorraine 2333) with a 10 mm inner diameter and then placed in the SPS machine to be treated. The annealing temperature, which was determined with a K-type thermocouple positioned within the graphite die and whose tip was situated 1 mm away from the sintered pellet, was set to 320 °C and maintained for 15 min under vacuum. The heating rate was monitored at 75 °C/min via a sequence of 1 pulse of 1 ms of DC polarization, while the applied pressure was 50 MPa. Upon cooling to room temperature, the dense pellet was recovered, scratched from any carbon traces, and ground prior to being X-rayed. The XRD powder pattern reveals the presence of sharp and intense peaks indicating the formation of a highly crystalline *triplite*. All the peaks were refined leading to unit cell parameters similar to those obtained for the phase prepared by either the dry or polymeric processes (Figure 7b). This is a straightforward confirmation that the formation of the *triplite* phase does not involve a *topotactic* reaction and therefore does not require water-containing precursors.

Ball Milling Synthesis. In addition to SPS, reactive ball milling was also explored. Ball milling has been intensively used in the field of Li battery research since the pioneering work of F. Disma back in 1996,[23,24] to either intimately combine active material/carbon composites for high-efficiency electrode utilization or to prepare numerous alloys pertaining to the Li_xSn, Li_xSi, and Li_xGa systems. The process involves repeated fracturing of powder particles in high-energy ball milling, which results in particle and grain size reduction together with the advent of structural defects. These lattice defects combined with short diffusion distances are believed to be the driving forces to promote low-temperature chemical reactions. Encouraged by the one-hour ball-milling mixing of our precursors for the SPS which has produced powders with a few extra broad Bragg peaks reminiscent of the *triplite* $LiFeSO_4F$, we have further pursued our ball milling experiments (denoted hereafter as BM). The BM experiments were performed using either a Spex 8000 mixer mill that generates normal mechanical strain or a Retsch PM200 mixer which provides planetary milling. The grinding vials having an open volume of 10 cm^3 were loaded and sealed in an argon drybox, using stainless steel balls to powder weight ratio ranging from 30 to 40, the powder being a mixture of stoichiometric amounts of $FeSO_4$ (made as described above) and LiF; grindings were done for times ranging from 1 to 6 h with a 10 min rest every 30 min to prevent excessive heating. After each grinding sequence, the powders were recovered and X-rayed to monitor phase evolution. We found that with a grinding time of 3 h and balls-to-powder weight ratio of 40 we could produce single-phased *triplite* $LiFeSO_4F$ powders, as all the peaks of their XRD powder pattern (Figure 7c) could be refined leading to unit cell parameters similar to those obtained for SPS or ceramic prepared phases. BM times exceeding 5 h were found to promote a beginning of amorphization. In contrast, we found that shorter BM times with balls to powder weight ratio of 40 or longer BM times with a ratio lower than 40 lead to an incomplete *triplite* formation. Last, keeping this ratio equal to 40, it is worth mentioning that pure *triplite* powders, with the same degree of crystallinity as before, can be obtained as well with a Retsch PM200 mixer, but with a longer grinding time (5 h). The need for this longer milling time does not come as a surprise. It is simply due to the fact that the Retsch PM200 mixer, which applies both normal and tangential strains, is less energetic than the Spex 8000. Whatever the type of apparatus used, a common feature to the BM-made powder samples lies

dx.doi.org/10.1021/ja3074402 | J. Am. Chem. Soc. 2012, 134, 18380−18387

in their XRD patterns (Figure 7c) which present broader peaks compared to samples made by either ceramic or SPS approaches. Bearing in mind that particle size and defects affect the width of Bragg peaks, this observation indicates that the BM powders, besides being more faulted, are highly divided. Through the use of the Scherrer formula, we deduced an average crystallite size of 40 nm in agreement with the SEM data (Figure 7c inset). Last, we experienced that the addition of 10−20% carbon as a part of the precursor mixture does not affect the final product. This turns out to be an attractive point for electrochemical performance, as it provides in situ carbon coating.

Such encouraging results led us to examine the effect of BM on the as-made *tavorite* powder. Using conditions identical to those previously mentioned (Spex mixer with a ball to powder ratio of 40), we found that it is feasible to convert *tavorite* into *triplite* at room temperature in 3 h while one week was necessary when using a 320 °C annealing process (see Supporting Information Figure 1). This clearly suggests that the ball milling process, and its fast introduction of disorder, kinetically enhances the *tavorite*−*triplite* transformation.

The electrochemical performances of SPS- and BM-prepared *triplite* $LiFeSO_4F$, the former having been ball milled with 20% w/w carbon black (SP), were tested vs. lithium in Li-half Swagelok cells between 4.5 and 2.5 V at a C/20 rate (1 Li in 20 h). The voltage composition curves are reported on Figure 7e,f, respectively, together with the $V = f(x)$ curve for a sample made by the classical 320 °C ceramic process (Figure 7d). Both ceramic and SPS samples show similar $V = f(x)$ profiles with an electrochemical activity, around 3.9 V, characteristic of the *triplite* polymorph. Nevertheless, the shape of the $V = f(x)$ curve differs noticeably between the BM sample (Figure 7f) and both SPS (Figure 7e) and ceramic (Figure 7d) samples with for the former a more sloping variation of the voltage with composition as expected from the highly divided nature of the BM sample as deduced by both the SEM pictures and the XRD data (Figure 7c). We should note that the average voltage is slightly lower (3.8 instead of 3.9 V), and presently, we do not have any explanation to account for this result. Last, the polarization is slightly larger for the BM sample, suggesting a more sluggish kinetics as compared to the other samples. This could be due to greater density of defects, and to check this point, we are presently studying the effect of various annealings on the shape, the polarization of the voltage composition curve, and on the value of the average redox voltage. However, although no specific care was taken in optimizing electrode formulation, our SPS and BM samples show comparable performances in the area of capacity and retention to our optimized ceramic sample, at least for the first 50 cycles, the maximum we have tried.

Besides such performances, it is appealing to report that $LiFeSO_4F$ can be made from abundant and low-cost elements at 320 °C in less than 20 min (SPS) or at RT in 3 h (BM). This makes *triplite* $LiFeSO_4F$ a serious contender to $LiFePO_4$, since it displays similar energy densities, as its lower capacity is compensated by its higher voltage, and a better taping density, as no carbon coating is required as opposed to $LiFePO_4$.

e. Generalization of the SPS Synthesis Approach. We recently reported the synthesis of novel Fe-based potassium fluorosulfate ($KFeSO_4F$)[15] and lithium iron sulfate ($Li_2Fe(SO_4)_2$)[16] electrode materials from dry solid-state reactions carried out in sealed quartz ampoules for times ranging from two to six days. It was then tempting to prepare these phases by SPS to assess the universality of such a synthesis technique. Its implementation turns out to be quick and easy. Indeed, using similar annealing temperatures to those previously defined to stabilize these phases, we could prepare pure $KFeSO_4F$ and $Li_2Fe(SO_4)_2$ in 15 and 10 min, respectively, as compared to a few days with other methods while preserving or improving their electrochemical performances (Figure 8).

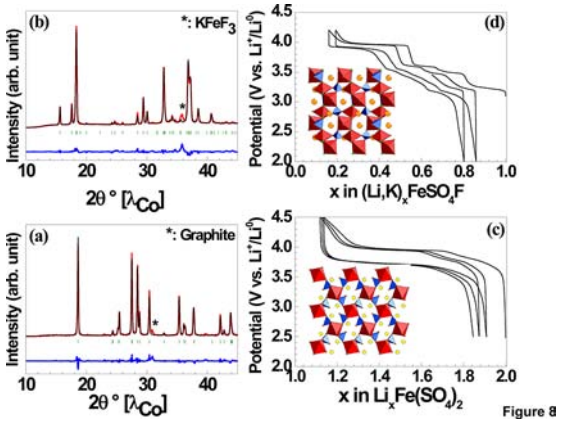

Figure 8. Rietveld refinements of XRD powder patterns of $Li_2Fe(SO_4)_2$ (a) and $KFeSO_4F$ (b) made from SPS synthesis. The stars indicate impurity peaks and correspond to graphite coming from the SPS matrix for $Li_2Fe(SO_4)_2$ and $KFeF_3$ impurity for $KFeSO_4F$. The corresponding electrochemical performances are displayed in (c) and (d). A reminder of their structure is displayed in the inset with the same color code as Figure 1, and K atoms are orange.

■ CONCLUSIONS

Understanding polymorphism presents unique opportunities to widen the knowledge of materials properties regardless of the field (e.g., superconductivity, magnetism, or redox potential); however, their stabilization as a single phase is frequently problematic owing to their nearly identical thermodynamic stability. Therefore, a prerequisite to stabilize a single-phased polymorph is the full understanding of their growth/nucleation path. Through various synthesis approaches coupled with XRD, SEM, and TEM measurements, we have provided practical means to reproducibly obtain both *tavorite* and *triplite* polymorphs with high purity. We confirmed that *tavorite* can reproducibly be formed at 300 °C either in sealed Teflon-lined autoclaves or under argon flow via a topotactic reaction from a mixture of $FeSO_4{\cdot}H_2O$ and LiF. Moreover, from both SPS and BM processes we have directly demonstrated the feasibility of preparing *triplite* $LiFeSO_4F$ from water-free precursors ($FeSO_4$ + LiF).

Besides obtaining *triplite* $LiFeSO_4F$ from dry precursors, another important finding deals with the ability to nucleate and grow the *triplite* phase from the *tavorite* via a long-heating treatment (a few days) at 320 °C with the observation that the kinetics of this transformation is enhanced in the presence of water traces. We show from TEM analyses (especially morphology of half way transformed particles) that this transformation was mainly controlled by a transport−diffusion process with its rate depending upon whether this process occurred through the bulk or in solution. Traces of water will enable transport via solution, which is quite a bit faster, therefore leading to faster kinetics as we observed.

dx.doi.org/10.1021/ja3074402 | J. Am. Chem. Soc. 2012, 134, 18380−18387

Overall, these experimental findings presented here are perfectly consistent with our earlier thermodynamic study from which we deduced, taking into account configuration entropies and enthalpy of formation, that the *tavorite*−*triplite* transition temperature should be 184 ± 69 K (Table 3 in ref 12). This indicates that, at typical synthesis temperature, the *triplite* phase is thermodynamically stable compared to *tavorite*. Moreover, this implies that the *tavorite* phase can only be prepared via a synthetic approach that kinetically favors its formation, and this is why it occurs only through a specific topotactic reaction involving the $FeSO_4{\cdot}H_2O$-related structure. Once formed, as expected from the thermodynamic results, *tavorite* converts slowly and irreversibly to the *triplite* phase at 320 °C. Therefore, at this stage, a legitimate question addresses the positive attributes of either ball milling or SPS processes to produce this phase by reacting $FeSO_4$ + LiF precursors either at room temperature (BM) or at 320 °C in 20 min (SPS), while the ceramic process requires 72 h at 320 °C. One believes that this difference is simply nested in the fact that both SPS and BM approaches are among the most efficient techniques to promote disorder so as to rapidly reach the necessary disorder to stabilize *triplite*. This is further supported by our ability to fully transform as made *tavorite* into *triplite* at RT in 3 h by ball milling, while it takes 6 days at 320 °C.

Finally, we still need to reconcile the above findings with our early work consisting in preparing *triplite* $LiFeSO_4F$ from $FeSO_4{\cdot}H_2O$ and LiF, provided that we use a quick heating to remove water so as to form $FeSO_4$ in situ, which then reacts with LiF in the presence of moisture. We believe that in this specific case water may indirectly help the reaction to proceed by facilitating the hydrolysis/dissociation of LiF, then enhancing reaction kinetics. Such a role is supported by our inability to trigger any chemical reactions by treating water-free ($FeSO_4$ + LiF) precursors under the same experimental conditions.

In conclusion, this work provides a new, important insight in the mechanism leading to the formation of *tavorite* and *triplite* $LiFeSO_4F$ polymorphs. It now enables the synthesis of most attractive 3.9 V $LiFeSO_4F$ polymorph either in a single step by directly reacting water-free precursors ($FeSO_4$ + LiF) via both SPS or BM techniques or via its nucleation−growth from the *tavorite* phase at 320 °C while preserving or even improving its electrochemical performances. Several improvements to the present work are immediately apparent and range from electrode optimization to a better control/measurement of the cationic disorder in these samples whether they are made by SPS or BM routes so as to establish a structural−electrochemical relationship. Last, by generalizing the SPS approach to the quick synthesis of other fluorosulfates ($KFeSO_4F$) and sulfates ($Li_2Fe(SO_4)_2$), we demonstrated its great versatility. As a whole, these insights point toward the positive attributes of both BM and SPS techniques in stabilizing new electrode materials, hence offering a new direction of research opportunity which goes well beyond the field of energy storage. The question therefore remains whether this technique, namely SPS, could present some economic advantages for mass production.

■ ASSOCIATED CONTENT

Supporting Information

XRD patterns showing formation of the *triplite* $LiFeSO_4F$ from *tavorite via* ball milling (Figure 1). This material is available free of charge via the Internet at http://pubs.acs.org.

■ AUTHOR INFORMATION

Corresponding Author

*E-mail: jean-marie.tarascon@sc.u-picardie.fr

Notes

The authors declare no competing financial interest.

■ ACKNOWLEDGMENTS

We would like to thank (i) V. Viallet and V. Seznec for giving us the opportunity to use SPS, (ii) J-N. Chotard and D. Larcher for fruitful discussions, (iii) R. Janot for his kind suggestions regarding ball-milling experiments, and (iv) A. Navrotsky for her expertise and insightful comments on thermodynamics.

■ REFERENCES

(1) Tarascon, J. M.; Armand, M. *Nature* **2001**, *414*, 359.
(2) Whittingham, M. S. *Chem. Rev.* **2004**, *104*, 4271.
(3) Padhi, A. K.; Nanjundaswamy, K. S.; Goodenough, J. B. *J. Electrochem. Soc.* **1997**, *144*, 1188.
(4) Nyten, A.; Abouimrane, A.; Armand, M.; Gustafsson, T.; Thomas, J. O. *Electrochem. Commun.* **2005**, *7*, 156.
(5) Sirisopanaporn, C.; Masquelier, C.; Bruce, P. G.; Armstrong, A. R.; Dominko, R. *J. Am. Chem. Soc.* **2011**, *133*, 1263.
(6) Yamada, A.; Iwane, N.; Harada, Y.; Nishimura, S.; Koyama, Y.; Tanaka, I. *Adv. Mater.* **2010**, *22*, 3583.
(7) Recham, N.; Chotard, J. N.; Dupont, L.; Delacourt, C.; Walker, W.; Armand, M.; Tarascon, J. M. *Nat. Mater.* **2010**, *9*, 68.
(8) Ati, M.; Melot, B. C.; Chotard, J. N.; Rousse, G.; Reynaud, M.; Tarascon, J. M. *Electrochem. Commun.* **2011**, *13*, 1280.
(9) Barpanda, P.; Ati, M.; Melot, B. C.; Rousse, G.; Chotard, J. N.; Doublet, M. L.; Sougrati, M. T.; Corr, S. A.; Jumas, J. C.; Tarascon, J. M. *Nat. Mater.* **2011**, *10*, 772.
(10) Ati, M.; Sougrati, M. T.; Recham, N.; Barpanda, P.; Leriche, J. B.; Courty, M.; Armand, M.; Jumas, J. C.; Tarascon, J. M. *J. Electrochem. Soc.* **2010**, *157*, A1007.
(11) Ati, M.; Walker, W. T.; Djellab, K.; Armand, M.; Recham, N.; Tarascon, J. M. *Electrochem. Solid State Lett.* **2010**, *13*, A150.
(12) Radha, A. V.; Furman, J.-D.; Ati, M.; Melot, B. C.; Tarascon, J.-M.; Navrotsky, A. *Journal of Materials Chemistry* [Online early access]. DOI: 10.1039/C2JM34071B.
(13) Tripathi, R.; Popov, G.; Ellis, B. L.; Huq, A.; Nazar, L. F. *Energy Environ. Sci.* **2012**, *5*, 6238.
(14) Taylor, G. F. Apparatus for making hard metal compositions. U.S. Patent 1896854, 1933.
(15) Recham, N.; Rousse, G.; Sougrati, M. T.; Chotard, J. N.; Frayret, C.; Sathiya, M.; Melot, B. C.; Jumas, J. C.; Tarascon, J. M. *Chem. Mater.* **2012**, DOI: 10.1021/cm302428w.
(16) Reynaud, M.; Ati, M.; Melot, B. C.; Sougrati, M. T.; Rousse, G.; Chotard, J. N.; Tarascon, J. M. *Electrochem. Commun.* **2012**, *21*, 77.
(17) Rietveld, H. M. *J. Appl. Crystallogr.* **1969**, *2*, 65.
(18) Rodriguez-Carvajal, J. *Physica B* **1993**, *192*, 55.
(19) Gerand, B.; Nowogrocki, G.; Guenot, J.; Figlarz, M. *J. Solid State Chem.* **1979**, *29*, 429.
(20) Figlarz, M. *Mater. Sci. Forum* **1994**, *152*−*153*, 55.
(21) Dumont-Botto, E.; Bourbon, C.; Patoux, S.; Rozier, P.; Dolle, M. *J. Power Sources* **2011**, *196*, 2274.
(22) Munir, Z. A.; Anselmi-Tamburini, U.; Ohyanagi, M. *J. Mater. Sci.* **2006**, *41*, 763.
(23) Aymard, L.; DelahayeVidal, A.; Portemer, F.; Disma, F. *J. Alloys Compd.* **1996**, *238*, 116.
(24) Salver-Disma, F.; Lenain, C.; Beaudoin, B.; Aymard, L.; Tarascon, J. M. *Solid State Ionics* **1997**, *98*, 145.